European Polymer Journal xxx (2012) xxx–xxx

Contents lists available at SciVerse ScienceDirect

European Polymer Journal

journal homepage: www.elsevier.com/locate/europolj

Macromolecular Nanotechnology

Effect of biaxial drawing on morphology and properties of copolyamide nanocomposites produced by film blowing

Emilia Garofalo *, Maria Letizia Fariello, Luciano Di Maio, Loredana Incarnato

Department of Industrial Engineering, University of Salerno, Fisciano (SA) 84084, Italy

ARTICLE INFO

Article history:
Received 29 May 2012
Received in revised form 18 September 2012
Accepted 27 September 2012
Available online xxxx

Keywords:
Polyamide-based nanocomposites
Film blowing
Biaxial drawing
Nanomorphology

ABSTRACT

In this work, extensional behavior in non-isothermal and isothermal conditions of copolyamide-based nanocomposites was analyzed and correlated to bubble stability in the film blowing processing of these materials. The higher values of transient extensional viscosity and melt strength of the nanocomposites, compared to the neat matrix, imply that they are able to better resist the extensional external force during bubble formation. Oxygen barrier and mechanical properties of the films were investigated and correlated to the resulting polymer crystal structure and filler morphology. At the higher draw ratios and blow up ratios the nanocomposite specimens were present essentially in the mesomorphic β-form, nevertheless, significant improvements in barrier and mechanical properties of the hybrid films were observed, likely due to a good dispersion and orientation of the silicate platelets in the polymer matrix.

1. Introduction

Plastic films can be made by both a flat and a tubular process. The tubular film blowing has the advantage over the flat film process in that the former produces biaxially oriented films, whereas the latter produces uniaxially oriented films. In general, the choice of one process over another is dictated primarily by the desired properties.

In the blown film process, a tube is formed and then, while it is molten, is blown up like a bubble to generate a large diameter tube from a relatively small circular die. The objective of the process is to produce a thin film having a uniform gauge and good mechanical, optical and barrier properties. In order to achieve satisfactory mechanical performances it is often advantageous, particularly in the case of packaging films, to have molecular orientation in the film that is more or less equal in the machine and transverse direction.

The weakness in the blown film process lies in the difficulty in achieving uniformity of the melt drawing process that occurs during the blowing. In particular, the shape and stability of the bubble are governed by the rheological properties of the polymer. Because of the complexity of the flow involved in the process, it is not easy to establish simple quantitative correlation between bubble stability and easily measured rheological properties. Moreover, during the film blowing process, non-isothermal conditions are realized and some structural effects, such as crystallization, appear only at solidification. Thus, an understanding of how both rheological and crystallization behavior can affect the processing and properties of blown films, is essential in order to achieve optimum results from this process. In particular, very few publications in the literature focus on production of polyamide layered-silicate nanocomposites by film blowing extrusion [1,2]. Several authors [3–7] found that thermo-mechanical treatments, during the production of bi-oriented nylon-6 films, induce remarkable variations of their structural microphase composition with significant effects on mechanical and transport properties. The addition of nanostructured layered silicate in nylon-6 strongly affect both rheological and

* Corresponding author. Tel.: +39 089 964024; fax: +39 089 964057.
E-mail addresses: egarofal@unisa.it (E. Garofalo), mfariello@unisa.it (M.L. Fariello), ldimaio@unisa.it (L. Di Maio), lincarnato@unisa.it (L. Incarnato).

0014-3057/$ - see front matter © 2012 Published by Elsevier Ltd.
doi:10.1016/j.eurpolymj.2012.09.024

Please cite this article in press as: Garofalo E. et al. Effect of biaxial drawing on morphology and properties of copolyamide nanocomposites produced by film blowing. Eur Polym J (2012), doi:10.1016/j.eurpolymj.2012.09.024

crystallization behavior of the polymer matrix [8–16], making fundamental the study of the processing-structure-properties relationship of polyamide nanocomposites produced by film blowing extrusion, in order to stabilize the process and control the developed morphology.

In this work, we analyze the effect of biaxial elongational flow, realized during a film blowing process, on morphology and properties of polyamide nanocomposite systems. In particular, a statistical copolymer of the nylon-6 (HADS), having a partially aromatic structure, was used as alternative matrix. The existence of stronger polymer–clay interactions in HADS nanocomposites than those of nylon-6 was demonstrated by several experimental data, reported in our previous works [8–11]. Nanocomposite systems at different silicate amounts were initially produced by melt compounding in a twin-screw extruder, to obtain satisfactory degree of silicate dispersion, and then submitted to single-bubble film extrusion. Hybrid films were collected at different blow up ratios and taking draw ratios.

2. Experimental

2.1. Film preparation

The silicate used in the preparation of the hybrids was Cloisite 30B (supplied by Southern Clay Products, Inc.), a layered sodium montmorillonite organically modified by methyl, tallow, bis-2- hydroxyethyl, and quaternary ammonium chloride (90 mequiv/100 g clay), having an interlayer basal spacing d_{001} = 18.5 Å.

A copolyamide of nylon-6 (denoted HADS and supplied by Caffaro SpA) was used as polymer matrix. The copolyamide investigated is made by random polymerization of ε-caprolactam in the presence of the comonomer 1,1″,3 trimethylcyclohexyl-3-methylamine-5-isophthalamide at 5 wt.%.

Nanocomposites pellets (at 3 and 6 wt.% of silicate amount) were initially prepared by melt compounding, and then used as feed for the following film blowing extrusion. The melt compounding, fundamental to achieve satisfactory degree of silicate exfoliation, was realized using a twin-screw extruder (L = 500 mm and L/D = 20) having counter-rotating intermeshing cone-shaped screws and, at the end of the extruder, a circular die with a diameter D = 2.5 mm. A temperature profile of 250-245-245-245 °C from hopper to die was imposed and a screw speed of 100 rpm was set. Prior to processing, the materials were dried in a vacuum oven at 90 °C for 18 h, resulting in a moisture level of less than 0.2 wt.%, in order to avoid polymer degradation during processing.

The effective level of organoclay into each extruded sample was determined by thermogravimetric analysis, which was carried out with a TGAQ500 (TA Instruments), from 25 to 900 °C at a thermal scan rate of 10 °C/min in air atmosphere. The amount of residue was corrected for the loss of organic component present in Cloisite 30B. Each determination was replaced on five specimens to obtain statistical silicate loading values.

Blown films were prepared using a Brabender DCE 330 single-screw extruder (L = 400 mm and L/D = 20), equipped with an annular die (30 and 32 mm inner and outer diameters, respectively). A temperature profile of 242–245–245 °C from hopper to die was imposed and a screw speed of 15 rpm was set. The films were collected at different blow up ratios (BUR = 2 and BUR = 2.5) and draw ratios (DR = 23 and DR = 35).

2.2. Characterization

Rheological experiments were conducted at 250 °C under a nitrogen atmosphere and after drying the samples at 90 °C for 18 h in a vacuum oven in order to prevent moisture induced degradation phenomena. Start-up shear flow experiments, with a cone and plate fixture, were performed with a Rheometric Scientific rotational rheometer, ARES (Advanced Scientific Expansion System) at a constant shear rate of 0.01 s^{-1}. The diameter of both the upper cone (cone angle = 0.1 radians) and the bottom plate was equal to 25 mm and a gap of 0.0533 mm was set. Rheological tests in elongational mode were carried out by using a Sentmanat Extensional Rheometer (SER) [17,18]. This instrument (model SER-HV-A01, manufactured by Xpansion Instruments) was designed for use as a detachable tool on ARES. Samples for testing were prepared by compression molding, using a preheated hydraulic press, and cut into small rectangles with the following dimensions: thickness, width and length of 0.8 × 6 × 15 mm, respectively, which were specifically chosen within the recommended ranges of sample dimensions for optimum instrument performance [17]. The elongational tests were performed at Hencky strain rates of 0.1, 0.3, and 0.5 s^{-1}, until the maximum achievable Hencky strain (equal to 3.8). The extensional viscosity of the neat matrix, used in the present work, resulted so low (<10^4 Pa s) that it was not possible to determine its accurate value at 250 °C using the SER extensional rheometer.

The fiber spinning experiments were conducted with a capillary rheometer (Rosand RH7, Bohlin Instruments) equipped with haul-off devices. The measurements were performed at 250 °C using a 1 mm diameter capillary die (L/D = 15). The molten polymer was extruded at a piston velocity of 5 mm/min and was drawn at different velocities until the filament broke.

Thermal analyses were carried out using a Mettler Differential Scanning Calorimeter (DSC30). An initial heating at 10 °C/min from 0 to 260 °C; an isotherm at 260 °C for 10 min to melt the residual crystals and remove the thermo-mechanical history; a cooling to 0 °C and a reheating to 260 °C at the same scan rate.

Transmission electron microscopy (TEM) analyses were conducted using a Philips EM 208 at different magnification levels. The images were captured on sections normal and parallel to the extrusion direction, which had been prepared by microtoming of ultra-thin specimens with a Leica Utracut UCT microtome.

Oxygen permeability of the films was determined with GPC-D Brugger permeability device at 30 °C according ASTM D1434 procedure.

Please cite this article in press as: Garofalo E. et al. Effect of biaxial drawing on morphology and properties of copolyamide nanocomposites produced by film blowing. Eur Polym J (2012), doi:10.1016/j.eurpolymj.2012.09.024

Mechanical tests were carried out, according to ASTM standard D882, by an Instron 4301. The films were tested with a grip distance of 40 mm and a crosshead speed of 5 mm/min to measure the Young's modulus and 50 mm/min to determine the stress and elongation at break.

The brightness of the films was measured by means of the colorimeter Chroma Meter CR-400/410 (produced by Konica Minolta) using the CIE Lab Colour Space that is more correctly known as $L^*a^*b^*$. The vertical L^* axis represents brightness, ranging from 0 (corresponding to a completely opaque sample) to 100 (corresponding to a transparent specimen). The other (horizontal) axes are represented by a^* and b^*. The a^* axis is green at one extremity (represented by −a), and red at the other (+a). The b^* axis is blue at one end (−b), and yellow (+b) at the other.

3. Results and discussion

3.1. Film blowing processability

Processability in the film blowing operation is very closely related to the molten state rheological behavior of the system. In particular, it is now well established [19–21] that the bubble instability problems are dictated by the elongational behavior of the polymer melt, as measured by its transient extensional viscosity (η_E^+).

The trend with time of η_E^+ for the copolyamide nanocomposite systems, studied in this work, was measured using the Sentmanat Extensional Rheometer (SER). The extensional viscosity of the neat matrix resulted so low (<10^4 Pa s) that it was not possible to determine its accurate value at 250 °C using the SER rheometer. However, 3-fold shear viscosity ($3\eta_0$) curve for the pure HADS copolyamide was plot in Fig. 1, where the elongational viscosity curves, as a function of time and at different Hencky strain rates, were also reported for 3% and 6% HADS hybrids. Analyzing the resulting η_E^+ vs time graphs (Fig. 1), it was observed that the nanocomposite samples show higher values of the extensional viscosity with increasing of silicate content and, conversely to the neat matrix, they show strain hardening behavior. As clearly evidenced by other authors [22], at Hencky strain rates in the range 0.1/0.5 s^{-1}, no strain hardening behavior exists in the neat polyamide matrix. These strain rates are not high enough for the primitive polyamide chain to extend and so this linear polymer does not show strain hardening phenomenon [22–24]. As reported in a recent study, carried out by our research group on the extensional behavior of polyamide-based nanocomposites [11], the peculiar extensional thickening of nanocomposites can be reasonably related to the presence of silicate platelets, which build up three-dimensional arrangements, the so-called "house of cards" structures, hindering extensional flow similarly to branches of the macromolecular chains. Strain hardening of extensional viscosity has been generally observed for long chain-branched polyolefines, and a correlation between the increasing strain hardening characteristics and improved bubble stability for LLDPE-rich blends was recently found in literature [25].

A rheological analysis in isothermal conditions may not be sufficient for a thorough investigation of film blowing processability, considering that some structural effects, such as crystallization, appear only at solidification. The non-isothermal elongational flow closely matches the

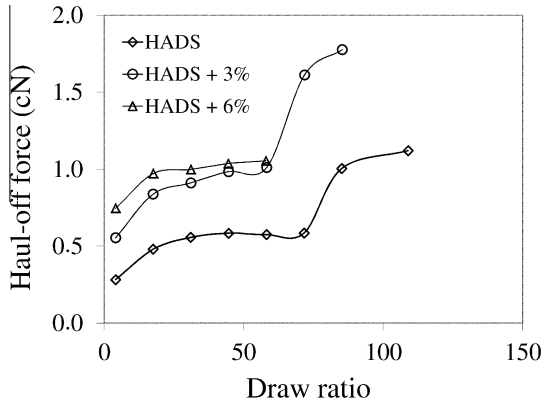

Fig. 2. Force-extensibility diagrams at 250 °C for the neat HADS matrix and HADS based nanocomposites at different silicate loadings.

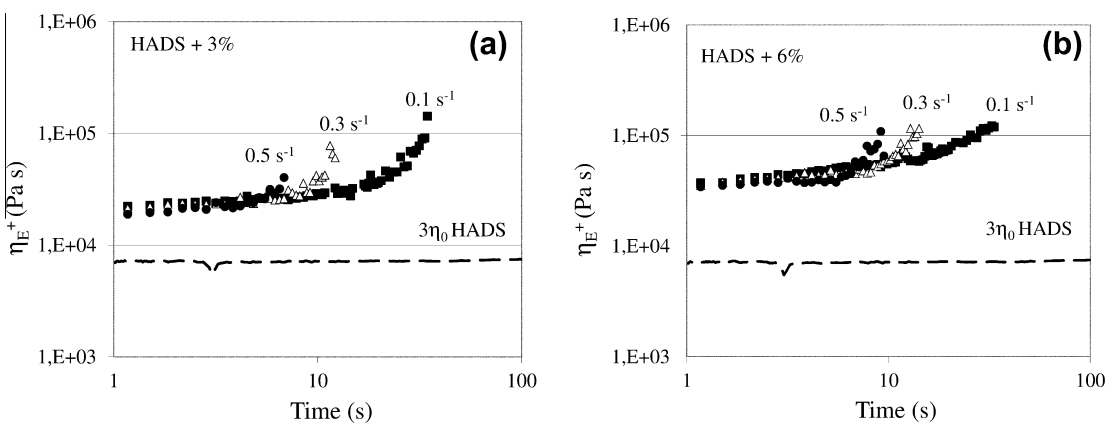

Fig. 1. Extensional viscosity profiles as functions of time at different Hencky strain rates: (a) 3 wt.% HADS nanocomposite and (b) 6 wt.% HADS nanocomposite. The dotted curve represents 3-fold shear viscosity for the neat copolyamide, taken at a low shear rate (0.01 s^{-1}) on a cone-plate rheometer.

Please cite this article in press as: Garofalo E. et al. Effect of biaxial drawing on morphology and properties of copolyamide nanocomposites produced by film blowing. Eur Polym J (2012), doi:10.1016/j.eurpolymj.2012.09.024

conditions experienced in film blowing process, and thus the measure of the Melt Strength (MS) and the Breaking Stretching Ratio (BSR) could give a very good indication of the film forming capability of the molten polymer systems.

Fig. 2 shows the force-extensibility diagrams for both copolyamide matrix and the hybrids at different silicate loadings. It can be seen that the drawdown force of the samples increases with the silicate loading, while the breaking draw ratio decreases with the clay concentration. Moreover, the neat matrix displays a strain-hardening phenomenon, reasonably related to the orientation of macromolecular chains along the stretching direction. Copolyamide based nanocomposites at lower silicate amount also retain strain hardening behavior, suggesting an orientation of the silicate platelets along the stretching direction and a good polymer–clay adhesion which facilitates the mechanical stress transfer to the reinforcement phase. At higher silicate content strain hardening is completely lost by the HADS hybrids, and melt deformability is seriously compromised. This behavior can be likely attributed to phenomena of filler aggregation inside the polymer matrix due to the stretching of the nanocomposites, particularly pronounced in the more loaded samples. The morphological analysis performed on the nanocomposite blown films, and reported in the following, confirms this hypothesis.

The filled materials are able to resist better to the extensional external force and then higher values of MS imply a good processability in processing operations like film blowing. The BSR values are slightly affected by the presence of the solid nanoparticles and significant differences can be observed only at the higher concentration (6 wt.%) of the filler. This feature is particularly interesting as the presence of a second, inert phase usually gives rise to a significant reduction of the melt stretchability that compromise the processability in those operations where elongational flow is involved. In this case, the nanoparticles, being well dispersed and having good adhesion with the matrix, do not act as ''defects'' in the molten polymer and no significant worsening of the melt deformability is revealed.

3.2. Effect of biaxial drawing on morphology and properties of the nanocomposite films

As expected from the rheological results, nanocomposite blown films were successful produced in a wide range of stretching conditions. In particular, hybrid films were collected at two different blow up ratios (BUR = 2 and BUR = 2.5) and draw ratios (DR = 23 and DR = 35), in order to study the effect of biaxial drawing on morphology and properties of the blown films. Optical, mechanical and oxygen barrier properties of the films were investigated and correlated to the resulting polymer crystal structure and filler morphology.

All the films exhibited a smooth texture that can be attributed to the acceptable levels of organoclay exfoliation, achieved in these nanocomposites, resulting from the use of an appropriate organoclay and optimum processing conditions. Moreover, the brightness (represented by the L^* parameter in the CIE Lab Colour Space) of the films was slightly compromised by the addition of the filler, in fact the values of L^* = 96.93 and L^* = 95.15 were measured respectively for the neat matrix and the hybrid at 6 wt.% of clay.

Morphological analyses, carried out by TEM microscopy on film sections normal to the extrusion direction, were performed to investigate the silicate dispersion inside the hybrid systems. Fig. 3a–d show TEM images of nanocomposite blown films obtained at different silicate contents and draw ratios. All the films were characterized by a mixed intercalated-exfoliated nanostructure with a satisfactory dispersion of the silicate on nanometric scale. However, a more uniform distribution of the clay platelets and a higher degree of silicate exfoliation were observed for the nanocomposite films with lower silicate amount and obtained at DR = 23 (Fig. 3a), whereas the more loaded and stretched samples displayed phenomena of silicate aggregation inside the polymer matrix (Fig. 3d). Recent studies [11,26], carried out by our research group on nanostructural arrangements induced by uniaxial drawing, has demonstrated that elongation flow can modify the nanomorphology of the hybrids, generally enhancing exfoliation degree and promoting orientation along the stretching direction, as also reported by other authors [27–29]. However, the application of high draw ratios, particularly in the case of the more loaded hybrids, can induce silicate aggregation due to the combination of reduced cross-area section upon stretching and face-to-face electrostatic interactions between adjacent silicate platelets [11].

In order to study the orientation distribution of the clay particles in the hybrid films, TEM analysis was also carried out on sections both parallel and normal to the film extrusion direction. In Fig. 4 the micrographs of 3 wt.% nanocomposite film at BUR = 2.5 and DR = 23, sectioned along the draw direction (MD) and perpendicular to the stretching direction (TD), are reported. The combination of these two images evidences that the clay layers slightly buckle perpendicularly to the draw direction. Compressive strain in the transverse direction arises from the Poisson effect, which results in decreased film thickness with increasing the deformation along the stretching direction [30]. In Fig. 5 the diameter of a curved nanoparticle is reported in detail.

The degree of platelet curvature has a significant influence on the effective aspect ratio of nanoclay. In particular, in terms of permeation properties, the curving of nanoplatelets shortens the tortuous path of the gas through the film. Moreover, any deviation from the arrangement, where silicate sheet planes lie parallel to the film surface, also leads to deterioration in gas barrier performance. On the other, in terms of mechanical properties, the orientation of silicate platelets inside the polymer matrix strongly affects the anisotropy degree of the nanocomposite systems.

At this regard, an accurate and semi-automatic image analysis was performed for all the nanocomposite samples in order to evaluate the orientation distribution (θ_x and θ_z distributions) of the exfoliated silicate platelets and intercalated clusters inside the hybrid films, (schematically represented in Fig. 6) as consequence of the induced orientation during the film blowing process. The morphological parameters of the nanocomposite films were evaluated by

Please cite this article in press as: Garofalo E. et al. Effect of biaxial drawing on morphology and properties of copolyamide nanocomposites produced by film blowing. Eur Polym J (2012), doi:10.1016/j.eurpolymj.2012.09.024

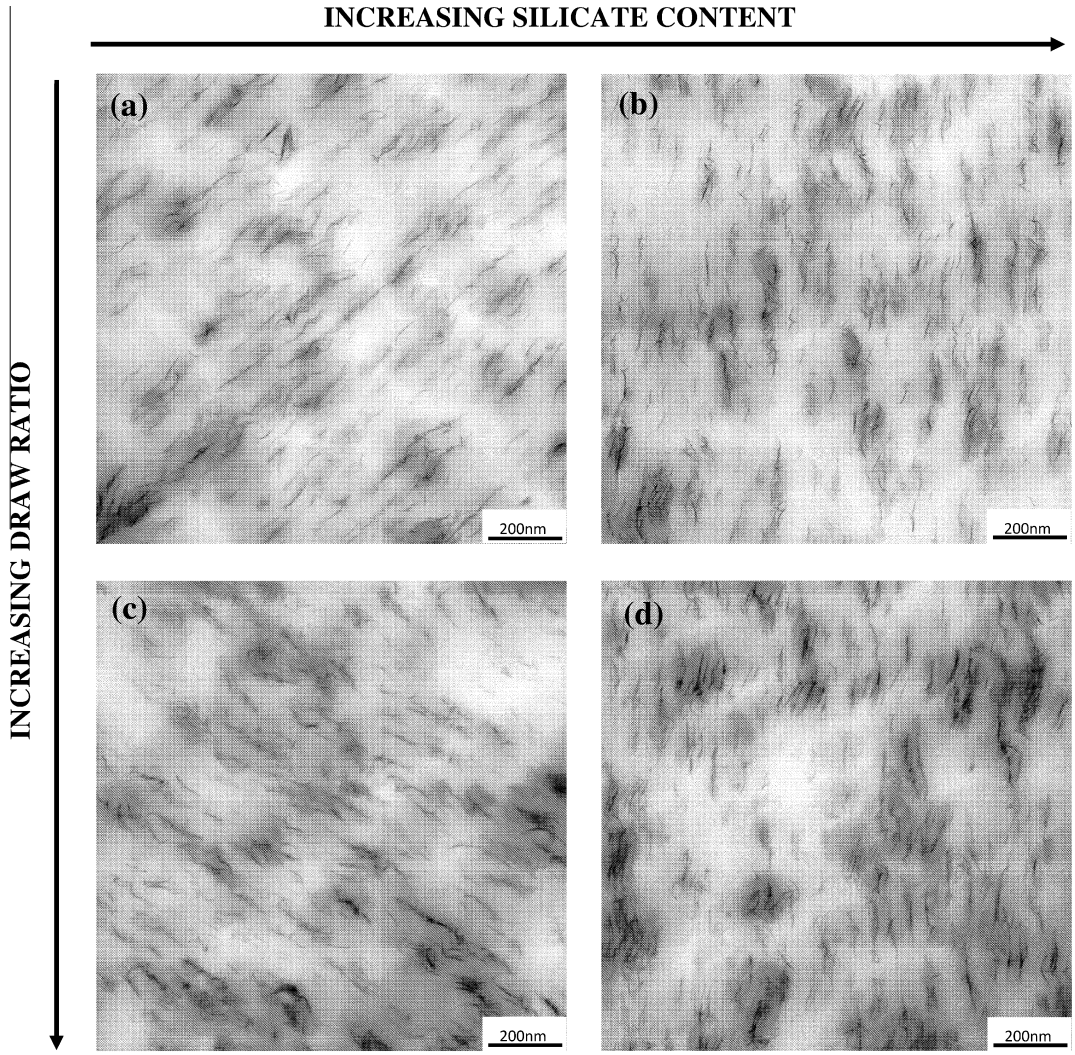

Fig. 3. TEM images of HADS nanocomposite films at fixed BUR = 2.5 and different silicate contents and draw ratios: (a) HADS + 3% at DR = 23; (b) HADS + 6% at DR = 23; (c) HADS + 3% at DR = 35 and (d) HADS + 6% at DR = 35.

following the method proposed by Vermogen et al. [31]. Images were taken at different magnifications in order to include in the analysis different types of clay platelets (individual sheets, thinner tactoids, thicker tactoids and agglomerates) to provide a good statistics of the distribution of the filler in the matrix. Around 300 tactoids/platelets were considered for each measurement. In Fig. 7 the frequency histograms, reporting θ_x and θ_z distributions for the hybrid film at 3 wt.% of silicate content and stretched at BUR = 2.5 and DR = 23, are reported, showing that the clay platelets are mainly oriented parallel to the film surface, as well as in all the nanocomposite samples analyzed.

To interpret properly the performances of the nanocomposite films, we have to take into account other factors affecting both mechanical and barrier properties, such as the degree of crystallinity and the crystal phases of the polymer matrix. Polyamides, in fact, exhibit three crystalline forms (α, γ and β) that generally coexist in various amounts, depending on processing conditions [6,7]. The α-phase is thermodynamically the most stable, the γ-phase is generally obtained under non isothermal crystallization conditions, and the β phase [6] is considered as a mesomorphic structure with random H-bond distribution and it is obtained under rapid cooling of polyamides from the melt.

At this regard DSC analyses were performed on all the samples and the first heating thermograms, related respectively to blown films at DR = 23 and DR = 35, being fixed the blow up ratio at BUR = 2.5, were reported in Fig. 8a and b. Analyzing the graphs in Fig. 8a, it clearly emerges that HADS film at DR = 23 is characterized by the α-crystal form (T = 214 °C). DSC thermograms of the nanocomposite films, stretched both at DR = 23 and DR = 35 (Fig. 8a and b), evidenced, instead, a broad exothermic peak in the range 150–200 °C, well above the glass transition temperature and just before the sharp endothermic peak at 214 °C. In agreement with the results of Penel-Pierron et al. [6,7], this

Please cite this article in press as: Garofalo E. et al. Effect of biaxial drawing on morphology and properties of copolyamide nanocomposites produced by film blowing. Eur Polym J (2012), doi:10.1016/j.eurpolymj.2012.09.024

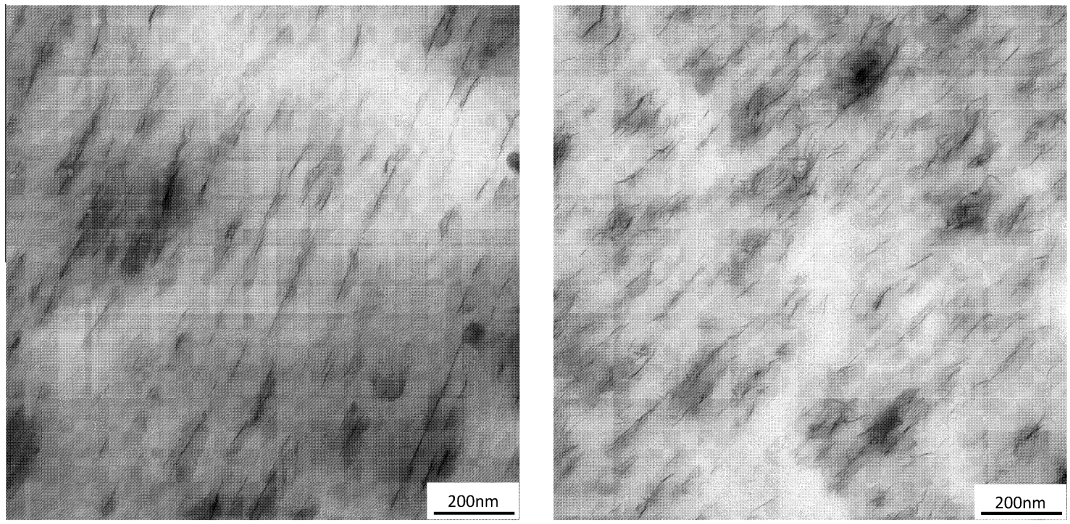

Fig. 4. TEM images of 3 wt.% nanocomposite film at BUR = 2.5 and DR = 23, sectioned (a) along the draw direction (MD) and (b) perpendicular to the draw direction (TD).

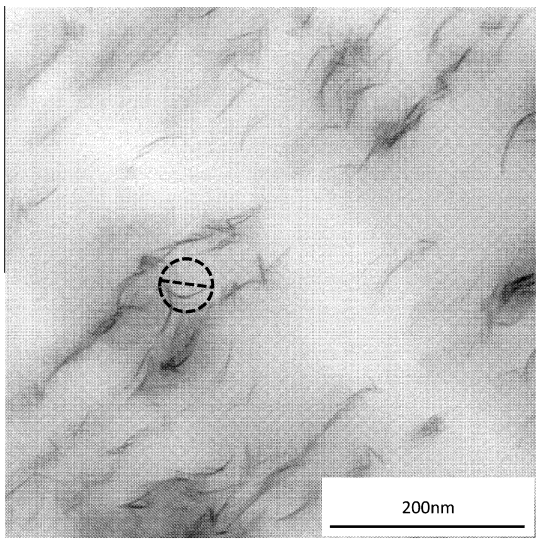

Fig. 5. Diameter of a curved nanoplatelet in the hybrid film at 3 wt.% of silicate content and collected at DR = 23 and BUR = 2.5.

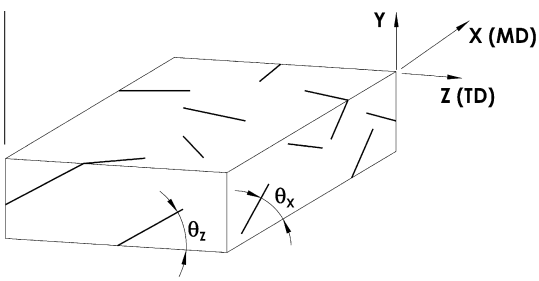

Fig. 6. Schematic view of spatial parameters (θ_x and θ_z) of the exfoliated silicate platelets and intercalated clusters in the nanocomposite films.

reorganization exothermic peak, during the heating scan, does not represent a recrystallization process, but it can be associated with an improvement of order from the mesomorphic β-phase into the stable α-phase. In the case of HADS nanocomposite films with 6 wt.% of silicate content (stretched both at DR = 23 and DR = 35) an additional exothermic peak occurs just before melting at about 180 °C (Fig. 8a and b). It can be reasonably attributed to the solid-state transformation into the α-form of a few unstable defective γ crystals. Moreover, HADS blown film stretched at DR = 35 was also obtained essentially in the mesomorphic β-form, which was induced by the fast cooling of the sample as a consequence of lower film thickness [6,7].

The mechanical properties of the neat matrix and nanocomposite systems were correlated to the resulting nanomorphology and crystal structures of the blown films. In particular, the competing development of the different crystal forms, more or less closely connected with the silicate platelets, in polyamide-based nanocomposites is likely to have a drastic incidence on the mechanical property improvements of the hybrid films.

The relative values of tensile properties (along the extrusion direction, MD) for the nanocomposite films with respect to neat HADS are compared in Fig. 9a–c by increasing the blow up ratio (Fig. 9a and b) and the draw ratio (Fig. 9b and c). At any stretching condition, the hybrid films showed better mechanical properties compared to the unfilled systems. In particular, the presence of the silicate leads to substantial improvements in stiffness, more pronounced in the case of blown films at BUR = 2.5/DR = 35. A reduction of the elongation at break is also shown by the nanocomposite systems. Furthermore, the mechanical properties of the nanocomposite hybrids at higher silicate content (6 wt.%) slightly increase (Fig. 9c) or even decrease (Fig. 9a and b) compared to 3 wt.% hybrids. These results may be attributed to the higher presence of nanofiller that favors nanoparticle face-to-face interactions leading to the formation of silicate aggregates (Fig. 3) in the more loaded samples.

Furthermore, the absolute values of the Young's modulus (both in machine MD and transverse TD

Please cite this article in press as: Garofalo E. et al. Effect of biaxial drawing on morphology and properties of copolyamide nanocomposites produced by film blowing. Eur Polym J (2012), doi:10.1016/j.eurpolymj.2012.09.024

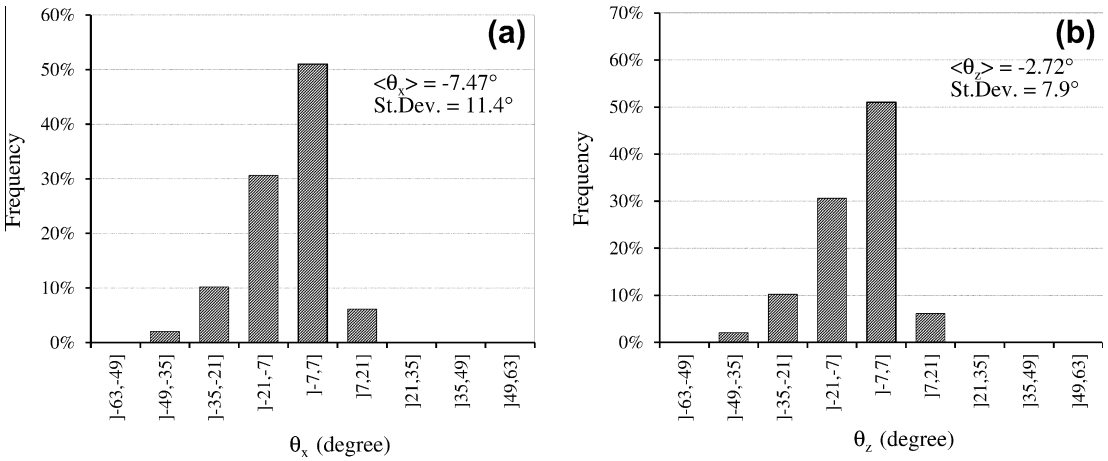

Fig. 7. Histograms of platelets spatial distributions for HADS blown film at 3 wt.% of silicate content and stretched at BUR = 2.5 and DR = 23: (a) θ_x distribution and (b) θ_z distribution.

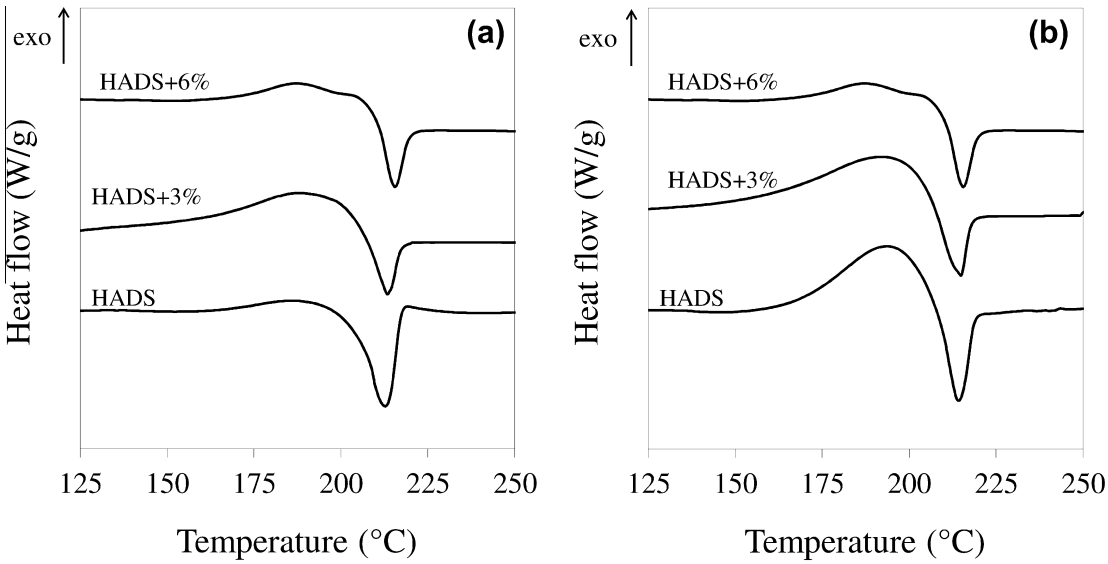

Fig. 8. First heating thermograms of HADS nanocomposite films blown at BUR = 2.5 and different draw ratios: (a) DR = 23 and (b) DR = 35.

direction) for the neat and nanocomposite films at different stretching conditions are reported in Fig. 10a and b. A reduction of the stiffness values can be observed for the films obtained at higher draw ratio and blow up ratio (Fig. 10a and b). These results can be attributed not only to silicate re-aggregation upon stretching but also to polyamide crystal phase changes during the single-bubble film blowing process. As evidenced by the thermograms reported in Fig. 8a and b, increasing the stretching conditions all the films exhibit essentially the mesomorphic β-form that is characterized by lower stiffness and tensile strength compared to the stable α-phase. Moreover, from Fig. 10b it can be observed that, increasing the blow up ratio at a fixed draw ratio (DR = 23), the rigidity of the samples becomes more or less equal in the machine and transverse direction, probably due to the enhanced orientation of the macromolecular chains in the TD direction.

The barrier properties, in terms of the oxygen permeability, of the neat matrix and nanocomposite systems were also investigated in order to complete the analysis of the film behavior. The permeability data, related to the nanocomposite films at a fixed blow up ratio (BUR = 2.5) and two different draw ratios, were reported in Fig. 11. All the nanocomposite systems show a decrease in oxygen permeability with respect to the neat matrix. Moreover, by comparing the permeability data of the hybrid samples at different draw ratios, it can be observed that nanocomposite films at DR = 23 exhibited better gas barrier properties than the corresponding hybrids collected at DR = 35. This feature was particularly pronounced in the case of the more loaded systems.

Please cite this article in press as: Garofalo E. et al. Effect of biaxial drawing on morphology and properties of copolyamide nanocomposites produced by film blowing. Eur Polym J (2012), doi:10.1016/j.eurpolymj.2012.09.024

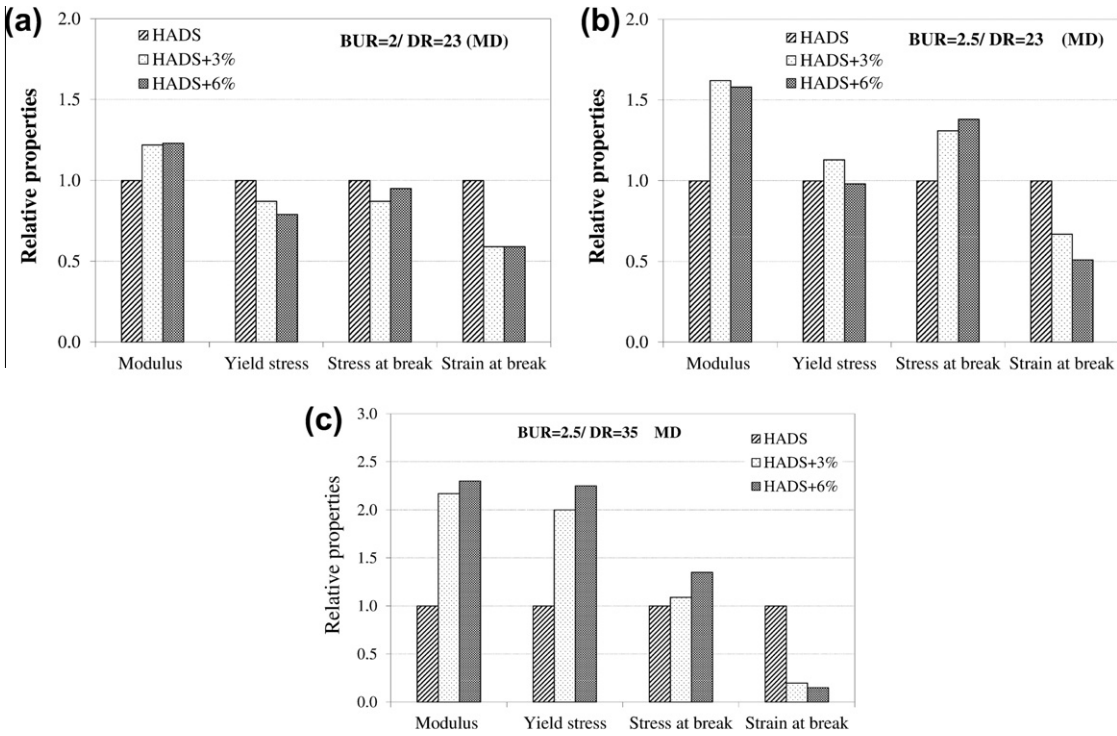

Fig. 9. Relative mechanical properties along the extrusion direction of the nanocomposite films compared to the neat matrix at: (a) BUR = 2/DR = 23; (b) BUR = 2.5/DR = 23; and (c) BUR = 2.5/DR = 35.

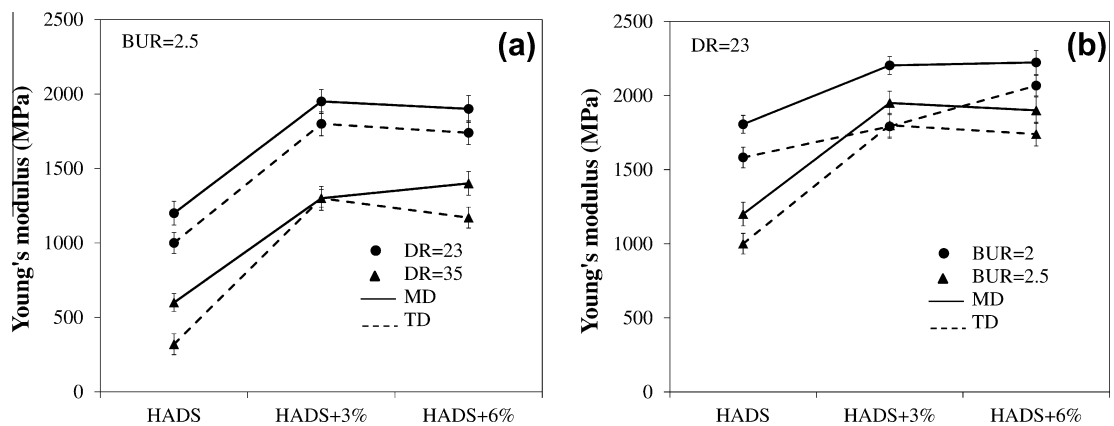

Fig. 10. Young's moduli in the machine (MD) and transverse (TD) direction of the neat matrix and nanocomposite films at different stretching conditions: (a) at a fixed blow up ratio BUR = 2.5 and (b) at a fixed draw ratio DR = 23.

Filler particles usually make two contributions to the barrier properties of nanocomposites. First, the fillers lengthen the travel path of the penetrants. Second, the matrix polymer properties, such as crystallinity and crystal phases are often altered in presence of fillers, thus affecting permeability. Based on the tortuous path models, it is clear that the aspect ratio of nanoplatelets has a significant effect on the permeation properties. In turn, the effective aspect ratio of nanoclay is greatly influenced by both the overall morphology of the silicate (degree of distribution and dispersion) and the morphology of the individual nanoplatelets (orientation and degree of curving) [32].

Concerning the crystalline structure, the HADS film at DR = 23 is characterized by the α-crystal form, while all the nanocomposite specimens exhibit the mesomorphic β-form, as evidenced by DSC thermograms in Fig. 8. In semi-crystalline polymers, the crystalline regions are considered to be gas impermeable [33], even if, in the case of polyamides, the mesomorphic β form, with variable degrees of disorder and stacking faults, is closed related to the amorphous phase from the standpoint of chain confor-

Please cite this article in press as: Garofalo E. et al. Effect of biaxial drawing on morphology and properties of copolyamide nanocomposites produced by film blowing. Eur Polym J (2012), doi:10.1016/j.eurpolymj.2012.09.024

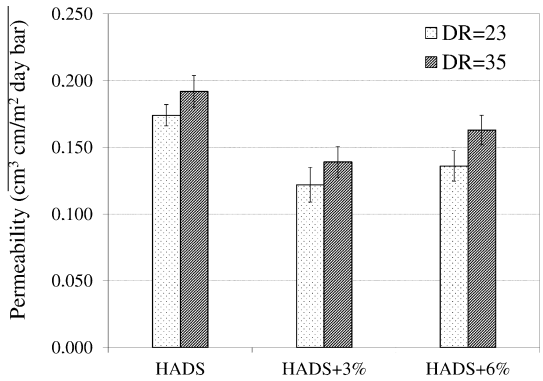

Fig. 11. Oxygen permeability data of HADS nanocomposite films at a fixed blow up ratio (BUR = 2.5) and two draw ratios (DR = 23 and DR = 35).

mation [6]. So the reduction in O_2 permeability of the nanocomposite films (Fig. 11) can be likely attributed to the presence of the silicate layers. In particular, the nanoclays appear to be well dispersed in the polymer matrix (Fig. 3) and show a preferential orientation along the extrusion direction (Fig. 7), as clearly evidenced by TEM analysis of the hybrid samples. Moreover, the worsening in gas barrier properties, observed in the more stretched and more loaded nanocomposite blown films, could be ascribed to the less dispersed nanomorphology and the increased degree of nanoplatelets curving (Figs. 3 and 4) compared with the corresponding films with lower silicate amount and obtained at lower draw ratio.

To quantify the levels of silicate exfoliation in the hybrid blown films stretched at different conditions, the permeability data were interpolated on the basis of the Nielsen theory [34] expressed by the following equation:

$$\frac{P}{P_m} = \frac{1-\phi_f}{1+\frac{\alpha}{2}\phi_f} \quad (1)$$

where P and P_m are respectively the permeability of the nanocomposite and the pure matrix, ϕ_f is the volume fraction of the filler, and α is its aspect ratio. In this simple model, based on the longer diffusive path that a gas must travel in the presence of filler, the reduction of permeability depends on the quantity of the filler and its aspect ratio. This means that, at fixed types and loading of silicate, the best gas barrier properties of a nanocomposite hybrid can be achieved by maximizing the aspect ratio, the structural parameter present in Eq. (1). Since the clay intrinsically has particles with a range of aspect ratios due to heterogeneity of arrangement on the nano and microscale, this parameter can be thought to be an average aspect ratio whose value is indicative of the degree of dispersion.

Applying Eq. (1) to the experimental data, the values of α, determined from the best fit, were 32 and 24, respectively, for the hybrid films stretched at BUR = 2.5 and DR = 23, and for the blown films at BUR = 2.5 and DR = 35. The calculated aspect ratios are in agreement with the TEM analysis performed on the nanocomposite samples (Fig. 3), showing a similar intercalated/exfoliated nanostructure for all the systems, even if a more uniform distribution of silicate platelets with smaller sized silicate aggregates can be observed for the film obtained at DR = 23.

TEM images at different magnifications were also used to evaluate empirically the average length-thickness ratio of silicate platelets-stacks and to compare with the aspect ratios based on the Nielsen model. The average aspect ratios obtained with the graphical approach [35] were 58 and 55 for the 3 wt.% hybrid films stretched, respectively, at BUR = 2.5 and DR = 23, and at BUR = 2.5 and DR = 35, higher than the values calculated by the Nielsen fit. This disparity can be explained in a number of ways. First, TEM images show small regions of the nanocomposite sample and for this, they may be not representative of the global nanostructure. Moreover, by using the graphical approach it was not possible to measure accurately the effective length of the exfoliated nanoparticles and the number of silicate platelets per stack because of the platelets curvature due to stretching. Finally, the Nielsen model considers a full exfoliation of the total amount of silicate present in each composite, therefore, only a lower volume fraction, corresponding to the well-exfoliated silicate fraction, should be considered in the Nielsen fitting.

4. Conclusions

In this work, the effect of biaxial elongational flow, realized during a film blowing process, on morphology and properties of copolyamide-based nanocomposites was analyzed.

The processing characteristics of the hybrid systems, produced by single-bubble film extrusion at different blow up ratios and draw ratios, were correlated to their extensional behavior in isothermal and non-isothermal conditions. The results, reported in this work, evidenced higher extensional viscosity and melt strength of the nanocomposite systems, compared to the neat matrix. Moreover, the breaking draw ratio values were slightly affected by the presence of the solid nanoparticles and significant differences were observed only at the higher concentration (6 wt.%) of the filler. The nanoparticles, being well dispersed and having good adhesion with the matrix, do not act as "defects" in the molten polymer and no significant worsening of the melt deformability was revealed, so copolyamide-based nanocomposite blown films were successful produced in a wide range of stretching conditions.

The brightness of the samples was slightly compromised by the addition of the filler, preserving an important property of the films in view of their use in packaging or other applications for which is fundamental to show the appearance of the packaged product.

Oxygen barrier and mechanical properties of the films were also investigated and correlated to the resulting polymer crystal structure and filler morphology, as consequence of different blow up ratios and draw ratios. At any stretching condition, the hybrid films showed better barrier and mechanical properties compared to the unfilled systems, due to the good dispersion and preferential orientation, parallel to the film surface, of the silicate platelets. In particular, the improved stiffness of the hybrid samples was associated to a decrease in film ductility that may

Please cite this article in press as: Garofalo E. et al. Effect of biaxial drawing on morphology and properties of copolyamide nanocomposites produced by film blowing. Eur Polym J (2012), doi:10.1016/j.eurpolymj.2012.09.024

represent a limit in some practical applications. This drawback can be overcome designing a proper multilayer structure where the copolyamide nanocomposite film has structural and barrier functions.

Moreover, a reduction of the stiffness values and oxygen permeability data was observed for the films obtained at higher draw ratio and blow up ratio. These results can be attributed not only to silicate platelet bending and filler reaggregation phenomena upon stretching, but also to polyamide crystal phase changes during the film blowing process. As evidenced by the thermal analysis, increasing the stretching conditions all the films exhibited essentially the mesomorphic β-form. This metastable crystal phase, with variable degrees of disorder and stacking faults, is closed related to the amorphous phase and it is characterized by lower stiffness and tensile strength compared to the stable α-phase.

References

[1] Dirama TE, Goettler LA. Film blowing of layered silicate nanocomposites. Mater Manuf Processes 2006;21:199–210.
[2] Beatrice CAG, Branciforti MC, Alves RMV, Bretas RES. Rheological, mechanical, optical, and transport properties of blown films of polyamide 6/residual monomer/montmorillonite nanocomposites. J Appl Polym Sci 2010;116:3581–92.
[3] Bianchi F, Cantagallo S, Consolati G, Laporta M, Pegoraro M, Tieghi G, et al. Properties of bioriented nylon 6 films related to film production technology. J Appl Polym Sci 2002;86:559–71.
[4] Rhee S, White JL. Investigation of double bubble tubular film extrusion of polyamide 6 and film structural characteristics. Polym Eng Sci 1999;39(7):1160–75.
[5] Rhee S, White JL. Crystal structure, morphology, orientation, and mechanical properties of biaxially oriented polyamide 6 films. Polymer 2002;43:5903–14.
[6] Penel-Pierron L, Depecker C, Séguéla R, Lefebvre JM. Structural and mechanical behavior of nylon 6 films part I. Identification and stability of the crystalline phases. J Polym Sci, Part B: Polym Phys 2001;39:484–95.
[7] Penel-Pierron L, Séguéla R, Lefebvre JM, Miri V, Depecker C, Jutigny M, et al. Structural and mechanical behavior of nylon-6 films. II. Uniaxial and biaxial drawing. J Polym Sci, Part B: Polym Phys 2001;39:1224–36.
[8] Incarnato L, Scarfato P, Scatteia L, Acierno D. Rheological behavior of new melt compounded copolyamide nanocomposites. Polymer 2004;45:3487–96.
[9] Incarnato L, Scarfato P, Russo GM, Di Maio L, Iannelli P, Acierno D. Preparation and characterization of new melt compounded copolyamide nanocomposites. Polymer 2003;44:4625–34.
[10] Russo GM, Simon GP, Incarnato L. Correlation between rheological, mechanical, and barrier properties in new copolyamide-based nanocomposite films. Macromolecules 2006;39:3855–64.
[11] Garofalo E, Russo GM, Scarfato P, Incarnato L. Nanostructural modifications of polyamide/MMT hybrids under isothermal and nonisothermal elongational flow. J Polym Sci, Part B: Polym Phys 2009;47:981–93.
[12] Baldi F, Franceschini A, Bignotti F, Tieghi G, Riccò T. Rheological behaviour of nano-composites based on polyamide 6 under shear and elongational flow at high strain rates. Rheol Acta 2009;48:73–88.
[13] Miri V, Elkoun S, Peurton F, Vanmansart C, Lefebvre JM, Krawczak P, et al. Crystallization kinetics and crystal structure of nylon6-clay nanocomposites: combined effects of thermomechanical history, clay content, and cooling conditions. Macromolecules 2008;41:9234–44.
[14] Xie S, Zhang S, Liu H, Chen G, Feng M, Qin H, et al. Effects of processing history and annealing on polymorphic structure of nylon-6/montmorillonite nanocomposites. Polymer 2005;46:5417–27.
[15] Esposito Corcione C, Maffezzoli A. Glass transition in thermosetting clay-nanocomposite polyurethanes. Thermochim Acta 2009;465:43–8.
[16] Calò E, Massaro C, Terzi R, Cancellara A, Pesce E, Re M, et al. Rotational molding of polyamide-6 nanocomposites with improved flame retardancy. Int Polym Proc 2012;27:370–7.
[17 Sentmanat M. Miniature universal testing platform: from extensional melt rheology to solid-state deformation behaviour. Rheol Acta 2004;43:657–69.
[18] Sentmanat M, Wang BN, McKinley GH. Measuring the transient extensional rheology of polyethylene melts using the SER universal testing platform. J Rheol 2005;49:585–606.
[19] Schlund B, Utracki LA. Linear low density polyethylenes and their blends: Part 5 extensional flow of LLDPE blends. Polym Eng Sci 1987;27(20):1523–9.
[20] White JL, Yamane H. A collaborative study of the stability of extrusion, melt spinning and tubular film extrusion of some high-, low-, and linear-low density polyethylene samples. Pure Appl Chem 1987;59(2):193–216.
[21] Dealy JM, Wissbrun KF. Melt rheology and its role in plastics processing. New York: Van Nostrand; 1990.
[22] Seong DG, Kang TJ, Youn JR. Rheological characterization of polymer-based nanocomposites with different nanoscale dispersions. e-Polymers 2005:005.
[23] Takahashi M, Isaki T, Takigawa T, Masuda T. Measurement of biaxial and uniaxial extensional flow behavior of polymer melts at constant strain rates. J Rheol 1993;37:827–46.
[24] Munstedt H, Laun HM. Elongational properties and molecular structure of polyethylene melts. Rheol Acta 1981;20:211–21.
[25] Micic P, Bhattacharya SN, Field G. Transient elongational viscosity of LLDPE/LDPE blends and its relevance to bubble stability in the film blowing process. Polym Eng Sci 1998;38:1685–93.
[26] Garofalo E, Russo MG, Di Maio L, Incarnato L. Study on the effect of uniaxial elongational flow on polyamide based nanocomposites. Macromol Symp 2007;247:110–9.
[27] Rajeev RS, Harkin-Jones E, Soon K, McNally T, Menary G, Armstrong CG, et al. Studies on the effect of equi-biaxial stretching on the exfoliation of nanoclays in polyethylene terephthalate. Eur Polym J 2009;45:332–40.
[28] Shah RK, Krishnaswamy RK, Takahashi S, Paul DR. Blown films of nanocomposites prepared from low density polyethylene and a sodium ionomer of poly(ethylene-co-methacrylic acid). Polymer 2006;47:6187–201.
[29] Koo CM, Kim JH, Wang KH, Chung IJ. Melt-extensional properties and orientation behaviors of polypropylene-layered silicate nanocomposites. J Polym Sci, Part B: Polym Phys 2005;43:158–67.
[30] Park S-Y, Cho Y-H, Vaia RA. Three-dimensional structure of the zone-drawn film of the nylon-6/layered silicate nanocomposites. Macromolecules 2005;38:1729–35.
[31] Vermogen A, Masanelli-Varlot K, Duchet-Rumeau J, Boucard S, Prele P. Evaluation of the structure and dispersion in polymer-layered silicate nanocomposites. Macromolecules 2005;38:9661–9.
[32] Mittal V. Barrier properties of poymer–clay nanocomposites. New York: Nova Science Publishers; 2010.
[33] Comyn J. Polymer permeability. London: Elsevier Applied Science Publishers; 1985.
[34] Nielsen LE. Models for the permeability of filled polymer systems. J Macromol Sci Chem 1967;A1:929–42.
[35] Cricrı' G, Garofalo E, Naddeo F, Incarnato L. Stiffness constants prediction of nanocomposites using a periodic 3D-FEM model. J Polym Sci, Part B: Polym Phys 2012;50:207–20.

Please cite this article in press as: Garofalo E. et al. Effect of biaxial drawing on morphology and properties of copolyamide nanocomposites produced by film blowing. Eur Polym J (2012), doi:10.1016/j.eurpolymj.2012.09.024